

# The Natural Patterns of Self-Cleaning Surfaces: RIMAPS Analysis of Superhydrophobic Leaves

Eduardo A. Favret<sup>1,2</sup> \* and Ana M. Molina<sup>3</sup>

<sup>1</sup> Instituto de Suelos, Instituto Nacional de Tecnología Agropecuaria (INTA), De Los Reseros y N. Repetto s.n., 1686, Hurlingham, Buenos Aires, Argentina

<sup>2</sup> Consejo Nacional de Investigaciones Científicas y Técnicas (CONICET), Av. Rivadavia 1917, C1033AAJ, CABA, Argentina

<sup>3</sup> Jardín Botánico "A. Ragonese", IRB, Instituto Nacional de Tecnología Agropecuaria (INTA). De Los Reseros y N. Repetto s.n., 1686, Hurlingham, Buenos Aires, Argentina

\* eafavret@cnia.inta.gov.ar

## Introduction

In the last decades, a new interdisciplinary science called biomimetics has emerged that has significantly influenced the design of certain new materials. Nature, as a source of inspiration, can give us ideas and concepts to implement new functional properties. One example is the self-cleaning property (superhydrophobicity) of certain plant leaves, better known as the Lotus Effect [1, 2]. This term comes from the lotus leaf (*Nelumbo nucifera*), the best-known self-cleaning surface in nature. On this kind of leaf, water droplets roll over the leaf surface and collect dirt and other particles from the surfaces. The superhydrophobicity of these leaves is caused, in general, by a hierarchical surface structure, built by a randomly oriented small hydrophobic wax structure on the top of convex cell papillae. The wetting condition of the solid surface is a particular property of materials and depends on both surface energy and surface topography. Many papers have been written to show how superhydrophobic surfaces with periodic and random patterns can be made, but few describe and characterize biological self-cleaning surfaces [3]. These papers usually analyze them by using optical profilers and scanning electron microscopy with specific sample preparation (for example, fixation) and in some cases atomic force microscopy. The main conclusion of those works is that binary structures (hierarchical microstructures and nanostructures) and unitary structures (basically nanostructures) are found in superhydrophobic plant leaves. However, no information regarding the general micro-nano structural pattern of biological surfaces on the  $x$ - $y$  plane has been reported. These surfaces seem to have a random pattern in most of the cases or at least a vague arrangement of its constitutive elements whose morphologies can be represented by geometrical figures (for example, hexagonal/pentagonal polygons, circles, and straight lines).

In the present work, the two-dimensional Fourier transform is introduced as a tool for describing the topographical pattern of the epidermis, which is composed of different features (for example, epidermal cells and papillae, which form the microstructure or micro-pattern, and epicuticular wax, which is the nanostructure or nano-pattern). This technique, called Rotated Image with Maximum Average Power Spectrum (RIMAPS), allows identification of the main directions of the micro-nano structural pattern and its distribution on the  $x$ - $y$  surface. This technique has recently been applied in the description of technological and biological surfaces [4–10]. Therefore, the aim of the present work is to describe, using RIMAPS, the micro-nano patterns of binary structures found

on superhydrophobic (ultra non-wettable) leaves, leaving for future work its comparison with non-wettable leaves.

## Materials and Methods

Leaves (fresh samples) from *Xanthosoma violaceum* Schott, *Oryza sativa* L., *Brassica oleracea* L., and *Tropaeolum majus* L. (Figure 1) were analyzed. We chose these species because they have sculptured leaf surfaces that are quite different. The static contact angles (CA) of these four leaves are between 155° and 165°, and the sliding angles are below 10°, which means they are superhydrophobic surfaces. Figure 2 shows a water drop lying on this kind of surface. A scanning electron microscope (FEI Quanta 200), low-vacuum, was used to obtain images of the morphology. In all cases, observations were made on the central part of the leaves, avoiding the main vein (see Figure 1).

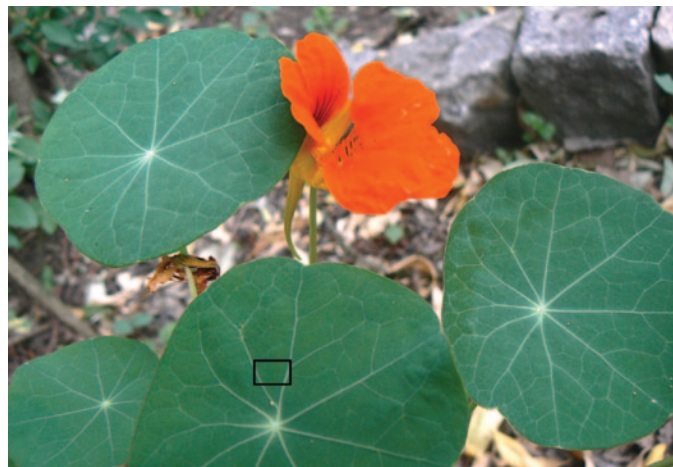


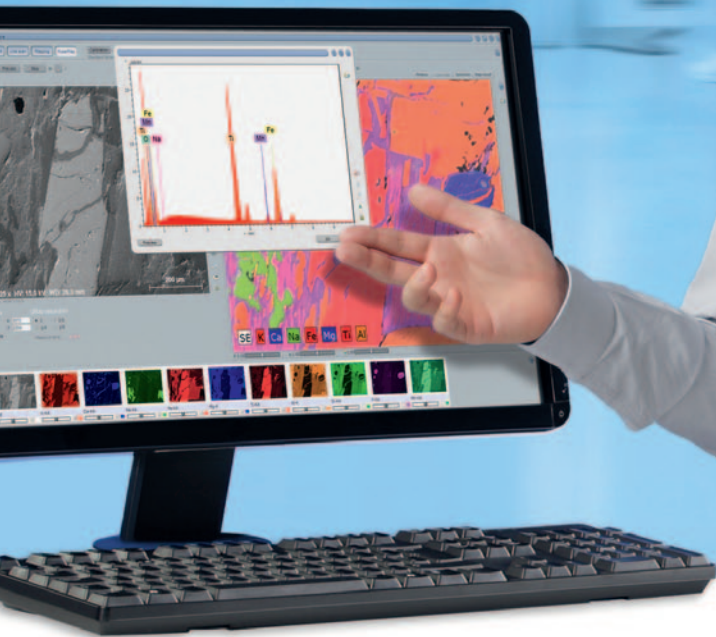
Figure 1. A *Tropaeolum majus* plant. The data were taken from the central part of the leaf (black box).



Figure 2. A water drop lying on a *Tropaeolum majus* leaf.



# QUANTAX – Ultimate EDS for SEM and TEM



- Data collection at the highest speed and at the best resolution you can get – first class results no matter the circumstance
- Excellent light element performance with  $\text{Mn K}\alpha \leq 123 \text{ eV}$  ( $\text{F K}\alpha \leq 54 \text{ eV}$ ,  $\text{C K}\alpha \leq 46 \text{ eV}$ ) even at 100,000 cps
- Best acquisition conditions for sensitive and rough samples through unique multi-detector systems and optimum geometry using VZ-Adapters
- Genuine standardless P/B-ZAF quantification for rough samples and VZ applications, Cliff-Lorimer quantification for TEM

[www.bruker.com/microanalysis](http://www.bruker.com/microanalysis)

The RIMAPS technique consists of rotating the image using algorithms of commercial software and calculating the  $x$ -step of the two-dimensional Fourier transform for each  $y$ -line of the new image obtained after rotation. As a consequence, averaged power spectra are obtained for each angular position. The corresponding maximum values are plotted as a function of rotation angle to obtain the RIMAPS spectrum. For a deeper explanation of this technique see reference 4. Basically, the peaks of the RIMAPS spectrum indicate the main angular directions of the topographic pattern and the arrangement of the micro and nano elements that constitute the leaf surface. Because for a full  $360^\circ$  rotation the RIMAPS spectra are symmetric, only the first  $180^\circ$  will be presented in the graphs.

## Results

The SEM images of *Oryza sativa* leaf (adaxial side) indicate a binary structure (microstructures and nanostructures) on its surface (Figures 3a and 3b). The microstructure is formed by the epidermal cells (think of them as rectangles), bumps, stomas, and prickles (see Figure 3b). The epidermal cells are located in a linear arrangement parallel to the apex (the longer side of the cell is parallel to the apex). All gramineae have this type of structure. The water droplets can roll off easily along the apex direction, but movement is much harder along the perpendicular direction. The differences between the two sliding angles ( $4^\circ$  and  $12^\circ$ ) are due to the anisotropic arrangement of the bumps [3]. The nanostructure is given by the epicuticular wax found between the bumps.

The RIMAPS spectra for both Figures 3a and 3b show an interesting difference (Figure 4). Whereas the RIMAPS spectrum of Figure 3a shows a main direction approximately in  $5^\circ$ – $10^\circ$ , which coincides with the apex direction, a secondary direction is found approximately in  $100^\circ$ – $110^\circ$  in the spectrum of Figure 3a, caused by the shorter side of the epidermal cells. In the case of Figure 3b, we have a higher magnification ( $2,000\times$ ), which means we are looking at a smaller area compared to the

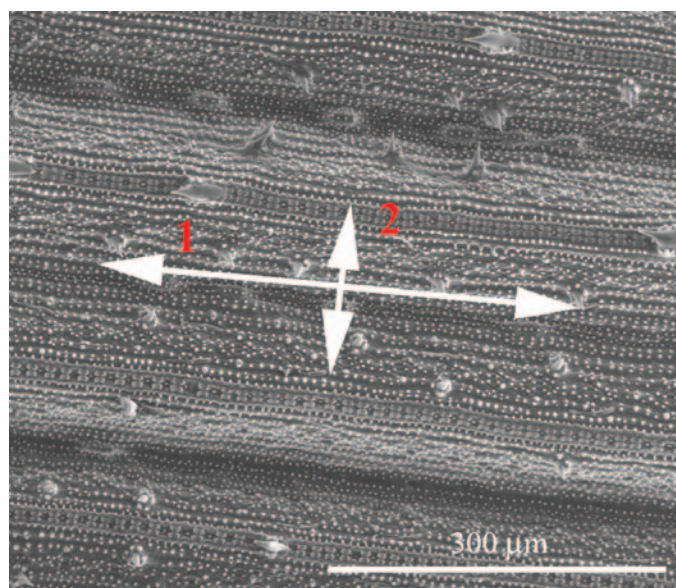


**Figure 3a.** SEM image of an *Oryza sativa* leaf. Arrows indicate the main direction (1) of the pattern, which coincides with the apex direction and its perpendicular (2). (Original magnification:  $500\times$ ).

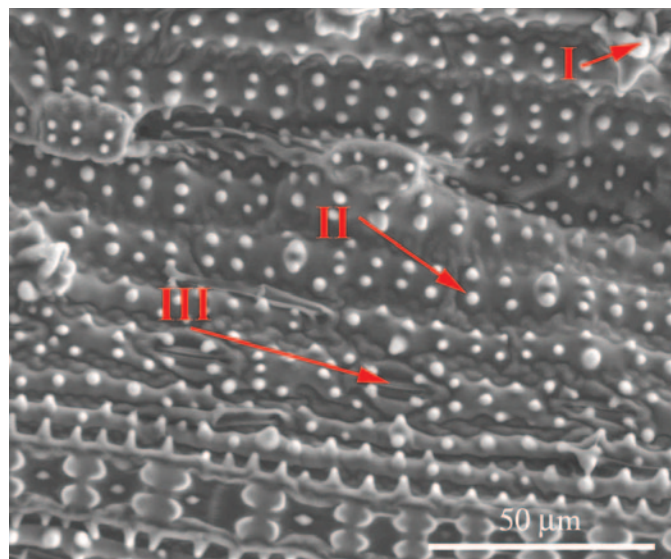


**Figure 3b.** Same sample as Figure 3a, but with a higher magnification. Prickles (I), bumps (II), and stomas (III) are seen (original magnification:  $2,000\times$ ).

previous case. The one-dimensional pattern that predominates in Figure 3a seems to disappear. The RIMAPS spectrum detects other angular directions, which were not clearly detected in Figure 3a ( $35^\circ$ ,  $65^\circ$ ,  $75^\circ$ ,  $120^\circ$ , and  $160^\circ$ ).

Figure 5 shows the microstructure of the *Tropaeolum majus* leaf (adaxial side), which also has a binary structure. The morphology and distribution of the epidermal cells are different from *Oryza sativa*. It has a convex epidermis, and there is more than one main direction of the pattern. The RIMAPS spectrum (Figure 6) coincides with this assumption for a  $400\times$  magnification. There are two global maxima, one around  $65^\circ$  and the other around  $130^\circ$ . If we magnify the visual field ( $1,600\times$ ), the maximum around  $130^\circ$  disappears, leaving only one global direction. It is important to point out that the width of these maxima at their base is between  $60^\circ$  and  $70^\circ$ , different from the case of *Oryza* with a base width of  $40^\circ$ .

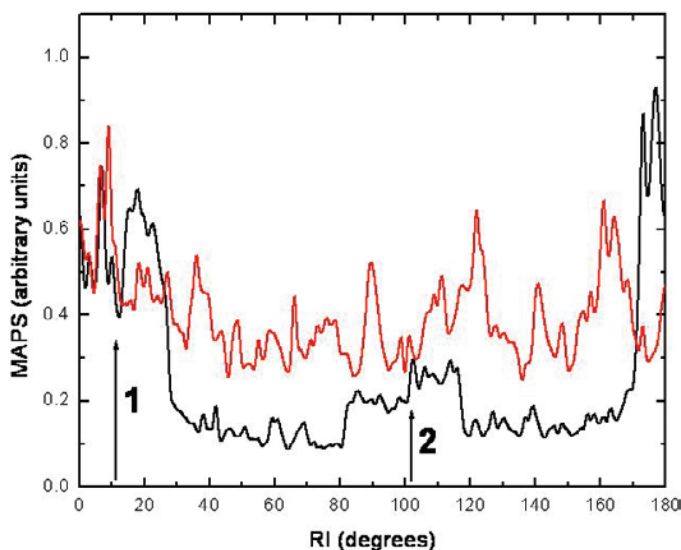


**Figure 4.** RIMAPS spectra of Figures 3a (black line:  $500\times$ ) and 3b (red line:  $2,000\times$ ). Arrows indicate the main direction of the pattern and its perpendicular.

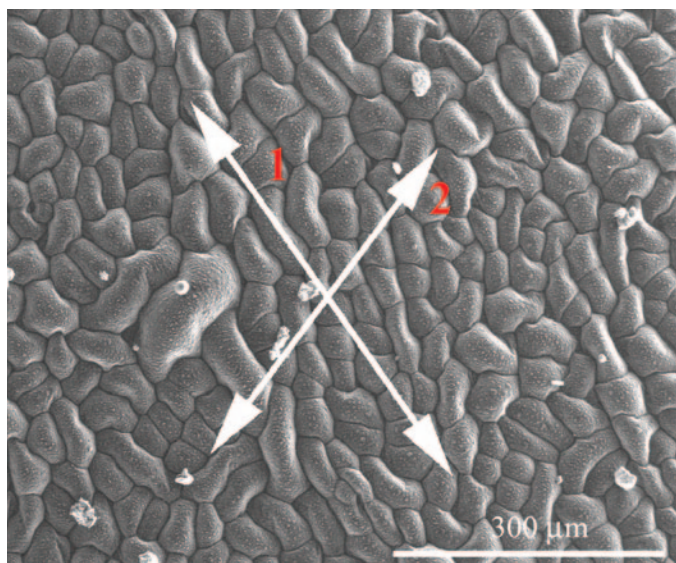


**Figure 5.** SEM image of a *Tropaeolum majus* leaf. Epidermal cells are seen. Arrows 1 and 2 indicate the two main directions of the pattern, obtained by RIMAPS (original magnification 400 $\times$ ).

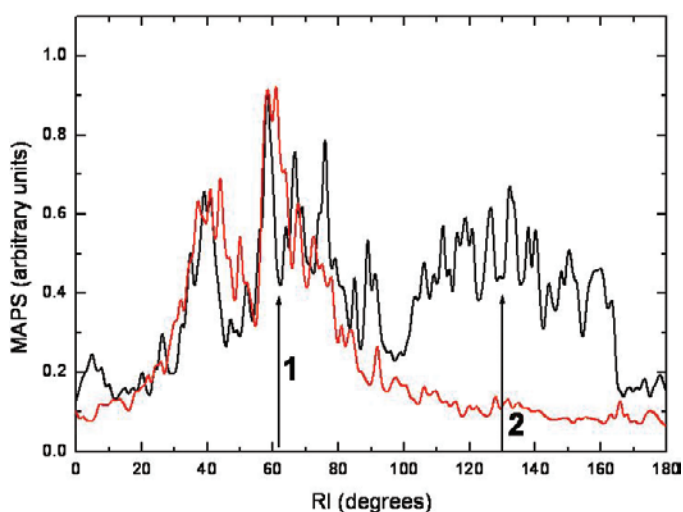


**Figure 6.** RIMAPS spectra of a *Tropaeolum majus* leaf with two different magnifications (black line: 400 $\times$ ; red line: 1,600 $\times$ ). Arrows 1 and 2 indicate the two main directions of the pattern, obtained by RIMAPS.

This is due to the more chaotic or isotropic arrangement of the epidermal cells of *Tropaeolum* compared to the case of *Oryza*. A less angular width of the maximum means a more linear pattern.

Figures 7 and 8 show the microstructure of *Xanthosoma violaceum* (abaxial side) and *Brassica oleracea* (adaxial side) leaves, respectively. The main characteristics of the topography of *Xanthosoma violaceum* are papillae, stomas, and wax, similar to the case of *Colocasia esculenta* and *Nelumbo nucifera*, which exhibit the Fakir effect (the drops sit on the top of the bed of micro-nano elements) [8, 11]. The peaks observed in the RIMAPS spectrum (Figure 9) are caused by the orientation of the arrangement of the micro elements of the surface. *Brassica oleracea* has a totally different microstructure. Its leaf surface has almost a planar cell sculpture, but it is densely covered with wax, which caused the Fakir effect. The amount and density of

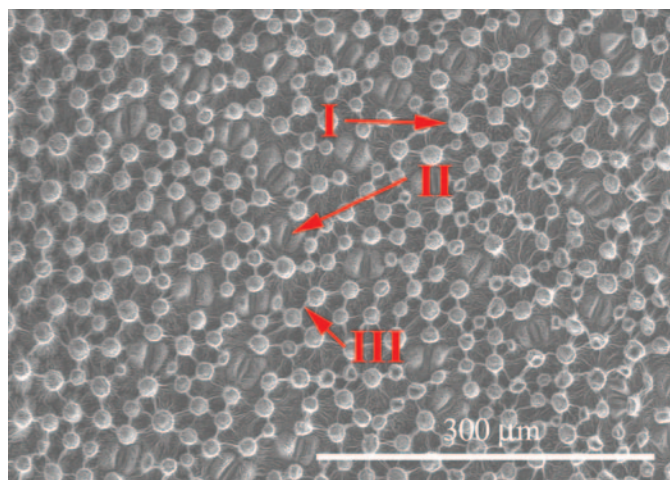


**Figure 7.** SEM image of a *Xanthosoma violaceum* leaf. Papillae (I), stomas (II), and epicuticular folders (III) are observed (original magnification: 500 $\times$ ).

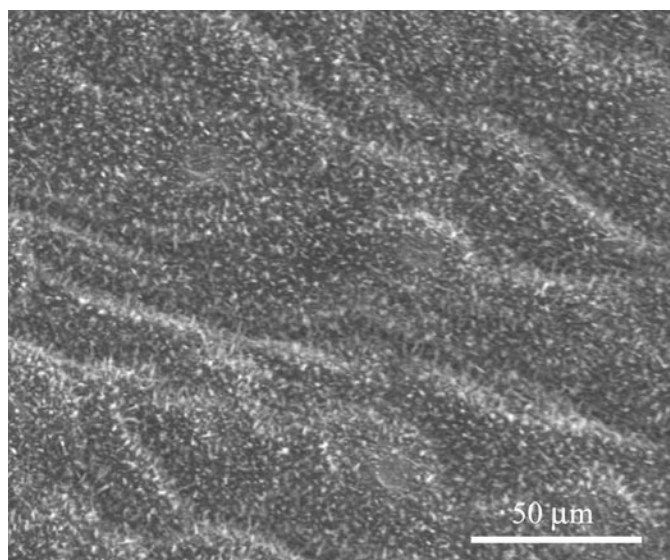


**Figure 8.** SEM image of *Brassica oleracea* leaf. Epicuticular wax is observed (original magnification: 1,600 $\times$ ).

wax is dependent on the humidity conditions in the air during cultivation [12]. The  $x$ - $y$  dimensions of the wax are below 1  $\mu\text{m}$ , which leads us to believe that in the case of *Brassica* we are dealing with a unitary structure instead of a binary structure. We used, in this case, a higher magnification, necessary to reveal the nanostructure. The RIMAPS spectra of *Xanthosoma* and *Brassica* are quite similar (Figure 9), indicating that the arrangement of the microstructure of *Xanthosoma* is almost equivalent to the nanostructure of *Brassica*. The RIMAPS spectrum of *Tropaeolum majus* is also compared to the spectra of *Xanthosoma* and *Brassica*, showing similarities in the angular range 40 $^{\circ}$ –160 $^{\circ}$ .

## Discussion

The species analyzed are superhydrophobic, and it is clear from the micrographs that the topography patterns of their leaves are not unique. However the existence of micro-nano elements on the surface seems to be a common characteristic between them, verifying the conclusion of previous works [2, 3]

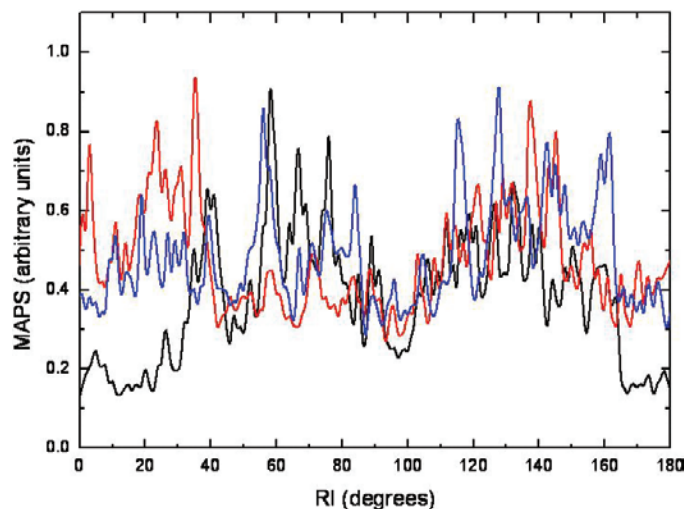


**Figure 9.** Comparison between the RIMAPS spectra of *Tropaeolum majus* (black line), *Brassica oleracea* (red line), and *Xanthosoma violaceum* (blue line) leaves.

that sculptured surfaces are needed to have a superhydrophobic condition. So far, the RIMAPS results of the biological species analyzed show that the distribution of the elements that constitute the microstructure and nanostructure of the leaf surface are quite similar, in spite of what we see on the micrograph. Perhaps this result goes beyond superhydrophobic leaves and is common to any type of leaf. In future research work, comparison with wettable leaf surfaces will be carried out.

More research needs to be done to answer questions such as “Is the topography pattern of superhydrophobic leaves a main element for having the self-cleaning condition?” We do not yet know the answer. However, we can imagine that the arrangement and size of the micro-nano elements of the surface are essential for having the self-cleaning condition.

The results show the robustness of RIMAPS analysis to distinguish and characterize the arrangement of the micro-nano patterns of leaf surfaces. This method is an auxiliary tool for the biologist to study surface variations of organisms. The use of RIMAPS opens a wide range of possibilities by providing tools for the quantitative description of leaf surfaces. In addition, this technique allows researchers to distinguish similarities and differences that occur in different environments and the quantitative parameters that represent an organismal lineage.

### Conclusions

The RIMAPS results obtained so far highlight the following conclusions: a) Different arrangements of micro-patterns are found on superhydrophobic leaves; b) For a given species, the topographical pattern shows differences depending on the size of the area studied; c) *Oryza sativa* has a linear micro-pattern for low magnifications; d) *Brassica oleracea* has a nano-pattern almost similar to the micro-pattern of *Xanthosoma violaceum*; e) The nano-pattern (epicuticular wax) seems to be isotropic, which means that the arrangement of the topographic features has multiple main directions.

### Acknowledgments

The authors wish to thank Dr. Patricia Bozzano and Mrs. Adriana Domínguez for their work on the scanning electron microscope.

### References

- [1] A Solga et al., *Bioinspiration & Biomimetics* 2 (2007) S126–S134.
- [2] K Koch, *Functional Nanoscience* in Proceedings of the International Beilstein Symposium on Functional Nanoscience by Beilstein-Institut, 2011, 167–78.
- [3] Z Guo and W Liu, *Plant Sci* 172 (2007) 1103–12.
- [4] N Fuentes and E Favret, *Journal of Microscopy* 206 (2002) 72–83.
- [5] E Favret et al., *Appl Surf Sci* 230 (2004) 60–72.
- [6] E Favret et al., *Microscopy Today* 12(5) (2004) 24–26.
- [7] E Favret et al., *Microsc Res Techniq* 69 (2006) 684–88.
- [8] E Favret and P Löthman, *Microscopy and Analysis* 21(1) (2007) 7–9.
- [9] E Favret et al., *Micron* 39 (2008) 985–91.
- [10] N Fuentes and E Favret, “RIMAPS and Variogram Characterization of Micro-Nano Topography” in *Functional Properties of Bio-inspired Surfaces: Characterization and Technological Applications*, eds. E Favret and N Fuentes, World Scientific Publishing, Jurong, Singapore, 2009, 155–79.
- [11] D Quéré and M Reyssat, *Philos T Roy Soc A* 366 (2008) 1539–56.
- [12] K Koch et al., *Environ Exp Bot* 56 (2006) 1–9.

MT

## PELCO® Silicon Nitride & Silicon Dioxide Membranes

### Next Generation SiN TEM Support Films

- Robust and clean 8, 15, 50 & 200nm SiN substrates
- ø3.0mm frame
- EasyGrip™ edges
- Free from debris
- Super flat 8, 15 and 40nm Silicon Dioxide Substrates



Holey SiN Substrates

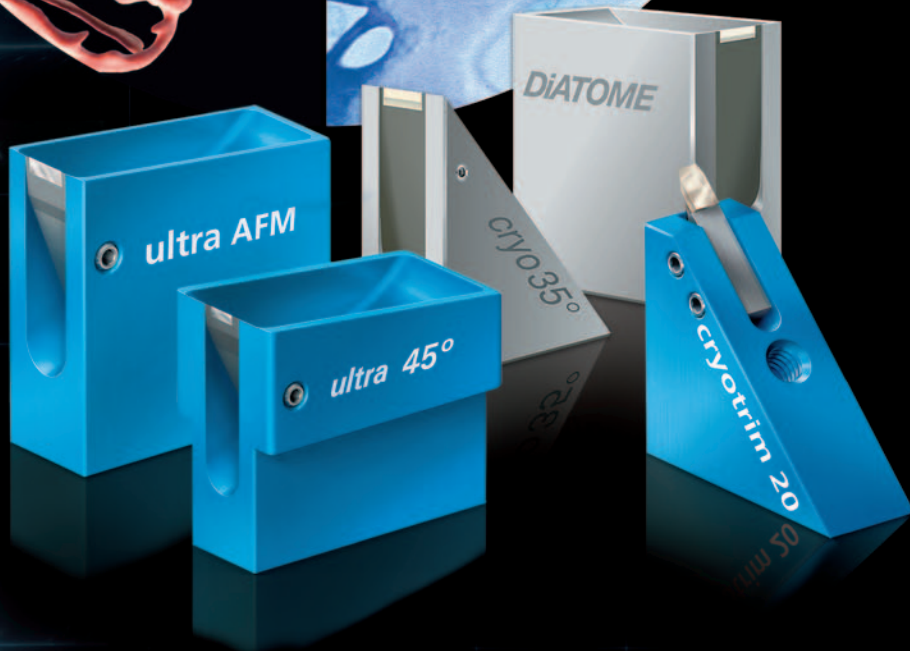
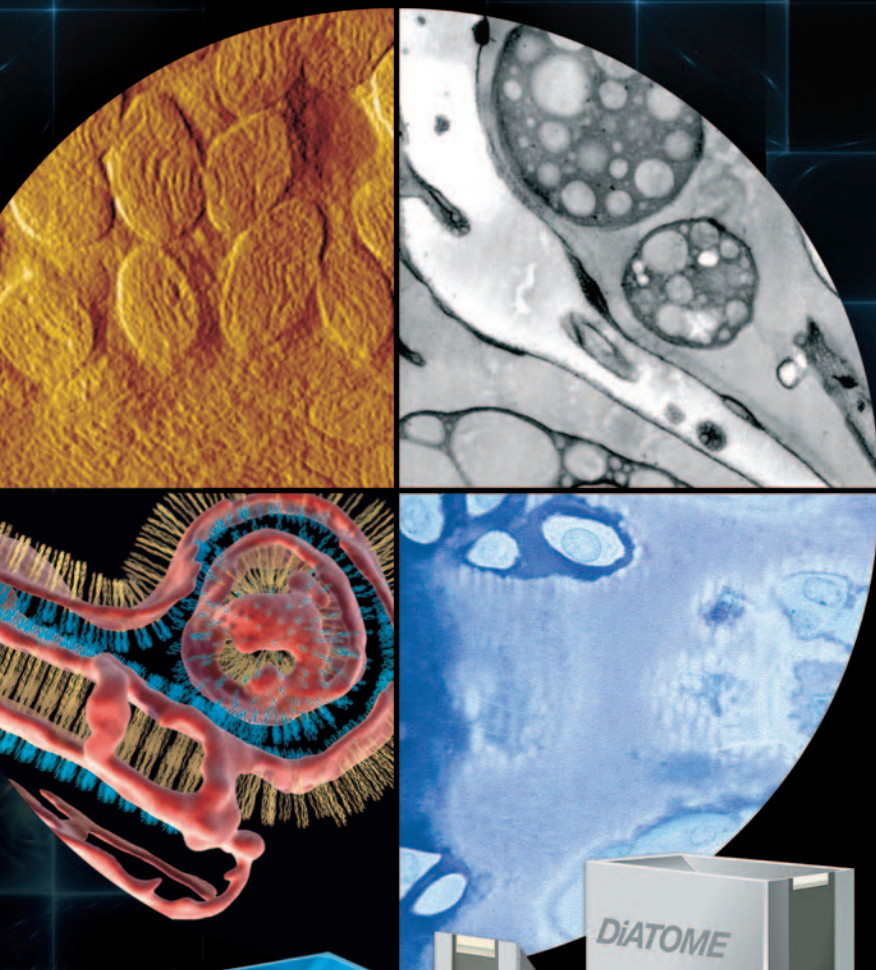


Silicon Dioxide Substrates

**TED PELLA, INC.**  
Microscopy Products for Science and Industry

sales@tedpella.com 800-237-3526 www.tedpella.com

**the highest quality...  
the most precise sectioning...  
incomparable durability**



#### **Free Customer Service**

Sectioning tests with biological and material research specimens of all kinds. We send you the sections along with the surfaced sample, a report on the results obtained and a recommendation of a suitable knife. Complete discretion when working with proprietary samples.

#### **Re-sharpening and Reworking Service**

A re-sharpened Diatome diamond knife demonstrates the same high quality as a new knife. Even knives purchased in previous years can continue to be re-sharpened. The knives can be reworked into another type of knife for no extra charge, e.g. ultra to cryo or 45° to 35°.

#### **Exchange Service**

Whenever you exchange a knife we offer you a new Diatome knife at an advantageous price.

40 years of development,  
manufacturing, and  
customer service

***DiATOME***  
diamond knives

ultra 45° • cryo • histo • ultra 35° • STATIC LINE II  
cryo-P • cryo immuno • ultra sonic  
cryotrim 45 and 25 ultra • AFM & cryo AFM • cryo 25°